Research Article | Vol. 28, No. 14 / 6 July 2020 / Optics Express 21072

Optics EXPRESS

Synthesizing quantum spin Hall phase for ultracold atoms in bichromatic chiral optical ladders

HANG YU,[1] EN GUO GUAN,[1,4] GANG WANG,[1,5] JIAN HUA JIANG,[1] JUN HU,[1] JIN HUI WU,[2] AND RAY KUANG LEE[3]

[1]School of Physical Science and Technology, Soochow University, Suzhou 215006, China
[2]School of Physics, Northeast Normal University, Changchun 130024, China
[3]Institute of Photonics Technologies, National Tsing-Hua University, Hsinchu 300, Taiwan
[4]1791920609@qq.com
[5]phwanggang@gmail.com

Abstract: Realizing the topological bands of helical states poses a challenge in studying ultracold atomic gases. Motivated by the recent experimental success in realizing chiral optical ladders, here we present a scheme for synthesizing topological quantum matter, especially the quantum spin Hall phase, in the chiral optical ladders. More precisely, we first establish the synthetic pseudo-spin-orbit coupling and Zeeman splitting in the chiral ladders. After analyzing the band structure of the ladders exposed to the bichromatic optical potentials, we report the existence of quantum spin Hall phase. We further identify a rich phase diagram of the bichromatic chiral ladders, illustrating that our proposal features a large space of system parameters exhibiting quantum phase transitions. Our scheme is within reach of the existing ladder optical lattices and hence provides a new method to engineer the elaborate topological bands for cold atomic gases.

1. Introduction

Identifying ways to search and probe topological optical lattices and thus topological quantum matter is a quest of major relevance in ultracold atoms [1,2]. Over the past decade, much progress has been witnessed in realizing the topological phases in cold atomic systems, ranging from the Su-Schrieffer-Heeger model [3], the Hofstadter model [4–6] to the Haldane model [7]. Important cases are the quantum spin Hall insulators (QSHIs) that arise in spin-orbit coupled systems, where the existence of helical edge states produces a spin current along the edges of a strip. Realizing the QSHI for ultracold gases was suggested in early theoretical works [8,9]. The QSHI would be implemented by engineering the hyperfine structure of the ultracold atoms to synthesize the non-Abelian gauge to mimic spin-orbit coupling [9]. On the experimental side, the only realized examples are cases where independent quantum Hall (QH) insulators of opposite Chern number have been paired to form a single system [5]. The system thereby is protected by a $\mathbb{Z}$ topological index. Despite these advances, optical lattices featuring QSHI with spin-orbit interaction have so far been lacking to our knowledge.

Along this line, chiral ladder systems for ultracold atoms constitute one of timely topics of engineering the topological quantum matter with synthetic gauge and synthetic dimensions [10]. They represent a simple yet effective platform to study exotic quantum phases of ultracold atoms, given that ultracold atoms in optical lattices naturally realize such a strip geometry [11]. Apart from the ladder structure in the real dimension [11], the internal degrees of freedom of atoms such as the hyperfine states [12,13] and clock states [14–16], and the external degrees of freedom such as the momentum states [17,18] and lattice orbitals [19,20], can be exploited to fabricate the chiral ladders in the synthetic dimensions. To date, an intense theoretical and experimental investigation has revealed rich topological features of the chiral ladders [10]. For example, the

#395756 https://doi.org/10.1364/OE.395756
Journal © 2020 Received 28 Apr 2020; revised 22 Jun 2020; accepted 25 Jun 2020; published 1 Jul 2020

Optics EXPRESS

chiral ladder systems in synthetic dimension have led to visualization of the chiral edge states related to the QH phase [12,13].

Motivated by these recent experimental realizations of ultracold atomic ladders immersed in synthetic gauge potentials [11–13], here we propose a chiral-ladder realization of the topological bands of QSHIs. To be specific, we utilize the leg degree of freedom to synthesize the pseudo-spin-orbit coupling and Zeeman splitting. By exposing it to a 1D bichromatic optical potential along the direction of legs, we develop a model of bichromatic chiral ladder. We analyze the energy bands of this bichromatic chiral ladder, revealing the quantum spin Hall phase. We further highlight the emergence of distinct topological phases by varying the parameters of the ladder systems. Our study is of direct experimental relevance for laboratories where ultracold gases in a chiral ladder geometry are realized [11–13,15–20], hence providing a realistic way to achieve topological quantum matter of ultracold atoms.

The rest of the paper is organized as follows. In Sec. 2 we construct the model of bichromatic chiral ladder. In Sec. 3 we calculate the energy bands and investigate the topological properties of the model, and finally summarize our results in Sec. 4.

2. Model of bichromatic chiral ladder

Our starting point is the ladder geometry of optical lattices for noninteracting *spinless* atoms that has been synthesized experimentally [11]. The access of QSHE at first requires the identification of two degrees of freedom representing the two spin states. We resort to a two-leg ladder threaded by a uniform artificial magnetic field [11], the so-called chiral ladder, to encode the two degrees of freedom and enable their mutual interactions. As sketched in Fig. 1(a), the chiral ladder consists of a two-leg strip with intra- and inter-leg hoppings J and K. Each plaquette encloses a net gauge flux 2ϕ. According to the Peierls substitution, the Landau gauge adopted here will imprint a phase factor $\pm i\phi$ on the hoppings along the legs ($\pm$ for the A- and B-legs, respectively). In addition, we superimpose an energy offset 2Δ between the legs. Physically, this offset corresponds to a deep double-well configuration oriented along the x direction. The overall ladder Hamiltonian in real space reads:

$$\begin{aligned}\mathcal{H} = &-J\sum_n \left(e^{i\phi}c^\dagger_{n+1,A}c_{n,A} + e^{-i\phi}c^\dagger_{n+1,B}c_{n,B} + \ h.c.\right)\\ &+\Delta\sum_n \left(c^\dagger_{n,A}c_{n,A} - c^\dagger_{n,B}c_{n,B}\right)\\ &-K\sum_n \left(c^\dagger_{n,A}c_{n,B} \ + \ c^\dagger_{n,B}c_{n,A}\right).\end{aligned} \tag{1}$$

Here the operator $c^\dagger_{n,\mu}$ ($c_{n,\mu}$) creates (annihilates) a fermionic particle on site (n,μ), where $\mu = (A,B)$.

A precise connection can be made between a spin-orbit coupled chain and the chiral ladder. Following the interpretation of Ref. [21], one can think of Eq. (1) as a 1D optical lattice with pseudo-spins represented by A- and B-legs. Keeping this in mind, we introduce the spinor operator $\Psi_n = \left(c_{n,A},\ c_{n,B}\right)^T$ and rearrange our model in the spinor space as follows:

$$\begin{aligned}\mathcal{H} = &\sum_n \Psi^\dagger_n \left[\Delta\hat{\sigma}_z - K\hat{\sigma}_x\right]\Psi_n\\ &-J\sum_n \Psi^\dagger_{n+1}e^{\imath\phi\hat{\sigma}_z}\Psi_n + h.c.,\end{aligned} \tag{2}$$

where $\hat{\sigma}_i$ are the Pauli operators. Written in the momentum-space the resulted Hamiltonian is of the form

$$\mathcal{H} = -\sum_{k_y}\Psi^\dagger_{k_y}M(k_y)\Psi_{k_y} \tag{3}$$

Optics EXPRESS

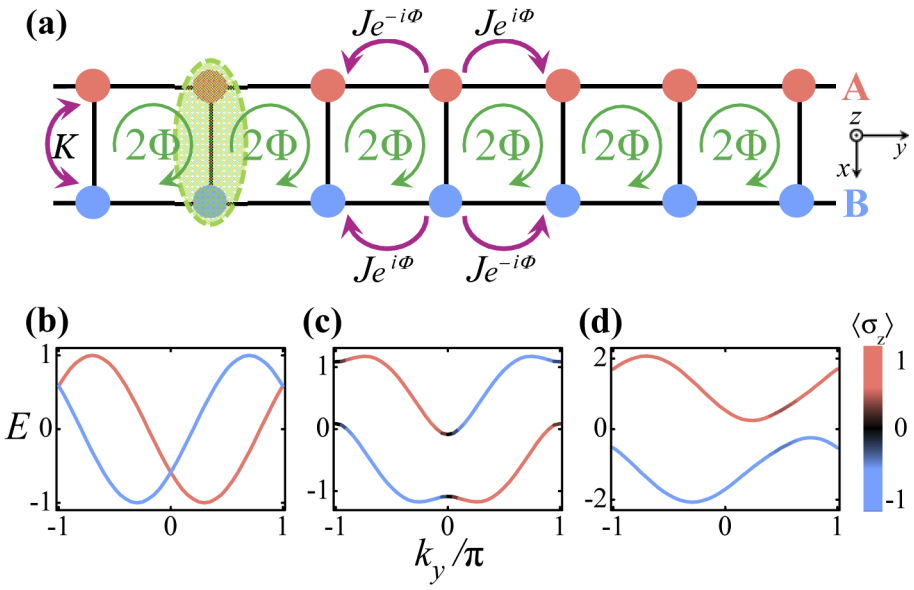

Fig. 1. (a) Schematic representation of the two-leg ladder. This optical lattice has a double-well structure in the x direction, while unlimitedly extends in the y direction. A and B (the red and blue colors) label the two different degrees of freedom of legs, denoting the two different pseudo-spin states. J and K are the hopping amplitudes along the legs and rungs, respectively. An artificial magnetic flux 2ϕ penetrates the plaquettes. An additional potential difference 2Δ is imposed between the legs. (b)-(d) Band structures of the chiral ladders for various K's and Δ's. Energy is set in units of $2J$. The color of the lines specifies the spin magnetization of the Bloch state. The magnetic flux is set as $2\phi = 0.6\pi$. Other parameters: (b)$K = 0,\ \Delta = 0$ (c) $K = 1,\ \Delta = 0$, (d) $K = 1,\ \Delta = 1$.

with $M(k_y) = 2J\cos\phi\cos(k_y)\hat{\sigma}_0 + \left[-\Delta + 2J\sin\phi\sin(k_y)\right]\hat{\sigma}_z + K\hat{\sigma}_x$. It should be noted that the 1D Hamiltonian has no chiral symmetry because of the first term proportional to the identity matrix. Besides that, we notice the absence of cosine term in the last two terms. This implies $\mathcal{H}$ is topologically trivial. We computed the energy bands and the pseudo-magnetization $\langle\sigma_z\rangle$ for a fixed flux 2ϕ and different values of inter-leg hopping K and energy offset 2Δ, shown in Figs. 1(b)–1(d). Figure 1(b) corresponds to the band structure in the case of vanishing K and Δ. Clearly, one can observe a positive (negative) shift of energy minimum for the pseudospin-up (-down) particles. This evidences an effective spin-momentum locking derived from the nonzero magnetic flux. Provided the inter-leg tunnelling K is turned on, as can be seen in Fig. 1(c), it opens a gap and the states get increasingly spin-mixed. Thereby the $\hat{\sigma}_x$ term in Eq. (3) brings about a spin-flip. Further, in the case of the large offset Δ a spin separation is visualized from the spin magnetization in Fig. 1(d). This term therefore indicates a pseudo-Zeeman splitting. In total, the above proposed chiral-ladder geometry can be mapped onto a 1D spin-orbit coupled lattice with spin flip and Zeeman field. It is necessary to stress that the pseudo-Zeeman term involved here is associated with the double well, instead of the artificial magnetic field. This is different from the electronic systems. As a result, it can give an independent control over the ladder systems.

To realize the topological bands of chiral ladders, we propose to impose a bichromatic optical superlattice $V(y) = V_p\cos^2(k_p y) + V_a\cos^2(k_a y + \theta)$ along the y direction. This can be created by superimposing on a primary, deep lattice an auxiliary, weak lattice [22]. V_p and V_a separately denote the depth of the primary and auxiliary lattices. k_p and k_a are the two lattice wave numbers.

Optics EXPRESS

The variable phase θ accounts for the relative position of the lattices. The bichromatic modulation is applied equally on the A- and B-legs (the shaded circle of Fig. 1(a)). When the primary lattice depth is sufficiently large, the wavefunctions can be expanded by a set of Wannier states $w(y)$ of the lowest band of the unperturbed primary lattice [23]. In the tight binding limit, this expansion leads to the onsite potential energies as follows $V(n) = \Lambda\cos(2\pi\beta n + \theta)$ [22]. Here, the modulation strength Λ is parameterized by the depth of the auxiliary lattice, β equals to the ratio k_a/k_p, and θ the phase offset. Summing up, the modulated optical ladder can be described by a tight-binding Hamiltonian

$$\begin{aligned}\mathcal{H}_{1D}(n,\theta) = &-\sum_n \Psi_n^\dagger\left[\Lambda\cos(2\pi\beta n+\theta)\right]\Psi_n\\ &+\sum_n \Psi_n^\dagger\left[\Delta\hat{\sigma}_z - K\hat{\sigma}_x\right]\Psi_n\\ &-\sum_n J\Psi_{n+1}^\dagger e^{\imath\phi\hat{\sigma}_z}\Psi_n + h.c..\end{aligned} \tag{4}$$

The first term describes the bichromatic modulation. In the second term Δ and K denote the strength of Zeeman splitting and pseudospin flip specified above. And the last term contributes to the spin-orbit coupling. In experiments, Λ and J can be controlled independently by varying the depth of the primary and auxiliary lattice potentials. θ can be tuned by the relative shift between the two lattices. Δ and K can be freely altered by tilting the double-well. This setting of optical lattices enables us to continuously tune the system among various topological regimes, as is elaborated below. Hereafter, the chiral ladders with the bichromatic modulation will be referred to as "bichromatic chiral ladders (BCLs)" for convenience.

3. Quantum spin Hall phase and topological phase diagram

In order to identify the topological nature of the BCL structure, we now establish the connection of the 1D BCL to a 2D spin-orbit coupled square lattice pierced by a magnetic field. The 2D Hamiltonian can be found by using the approach of dimensional extension [24–28]. To be specific, given the parameter θ is cyclically varied in $[0,\ 2\pi]$, it can be regarded as a quasi-momentum k_z along a virtual coordinate z. After making the substitutions of $J \to t_y$, $\theta \to k_z$, and $\Lambda \to 2t_z$ and relabeling the spinor as Ψ_{n,k_z}, the present 1D model can be converted into a 2D Hamiltonian in a mixed momentum-position representation $(n,\ k_z)$,

$$\begin{aligned}\mathcal{H}_{2D}(n,k_z) = &-\sum_{n,k_z} \Psi_{n,k_z}^\dagger\left[2t_z\cos(2\pi\beta n+k_z)\right]\Psi_{n,k_z}\\ &+\sum_{n,k_z} \Psi_{n,k_z}^\dagger\left[\Delta\hat{\sigma}_z - K\hat{\sigma}_x\right]\Psi_{n,k_z}\\ &-\sum_{n,k_z} t_y\Psi_{n+1,k_z}^\dagger e^{\imath\phi\hat{\sigma}_z}\Psi_{n,k_z} + h.c..\end{aligned} \tag{5}$$

Performing the inverse Fourier transform, $\Psi_{n,k_z} = \sum_m e^{-ik_z m}\Psi_{n,m}$, gives the real-space 2D Hamiltonian

$$\begin{aligned}\mathcal{H}_{2D}(n,m) = &-t_z\sum_{n,m} e^{\imath 2\pi\beta n}\Psi_{n,m+1}^\dagger\Psi_{n,m} + h.c.\\ &+\sum_{n,m} \Psi_{n,m}^\dagger\left[\Delta\hat{\sigma}_z - K\hat{\sigma}_x\right]\Psi_{n,m}\\ &-\sum_{n,m} t_y\Psi_{n+1,m}^\dagger e^{\imath\phi\hat{\sigma}_z}\Psi_{n,m} + h.c..\end{aligned} \tag{6}$$

Optics EXPRESS

This Hamiltonian exactly describes a spinor moving on a square lattice defined in the $y-z$ plane ($y=n, z=m$), which is threaded by a uniform magnetic flux β per plaquette. Based on the analogy between our 1D system and the 2D system, this allows us to define the topological properties of the BCL. That is the topological origin of our model. We should emphasize that, different from the conventional Harper-Hofstadter model [29,30], the terms associated with the spin-orbit coupling, spin flip, and Zeeman splitting are involved in the Hamiltonian Eq. (6).

Having precisely mapped the 1D BCL onto the analogous 2D system, we at this point move to the topological phases of the BCLs. Herein, we assume a rational β, i.e., $\beta=p/q$ with $p,\ q$ being coprime integers. The length of unit cell of the ladder turns out to be q. Inserting the Bloch waves $\Psi_{n+q}=e^{ik_y}\Psi_n$ in Eq. (4) yields the band structures $E=E(k_y,\theta)$ of the modulated ladder, together with the associated eigenvectors, that are defined by θ. Figure 2(a) displays the energy bands for $\beta=1/3$. To quantify the topological properties of our system, we calculate the spin-up (spin-down, respectively) gap Chern numbers defined in the parameter space (k_y,θ). In Fig. 2(a) we have labeled the spin gap Chern numbers. We note that for the middle gap the Chern numbers are given by $(C_\uparrow,\ C_\downarrow)=(-1,\ +1)$. This leads to the nontrivial topological index $\frac{1}{2}(C_\uparrow-C_\downarrow)=-1$ which signals the emergence of QSHI. It should be noted that the time-reversal symmetry is broken in the analogous 2D Hamiltonian, and thus this phase corresponds to the time-reversal-symmetry-broken QSHI phase [31]. In the meanwhile, the Chern numbers of the first gap are $(C_\uparrow,\ C_\downarrow)=(0,\ -1)$. This indicates a spin-filtered QH phase [32,33]. A similar result holds for the third gap, but with $(C_\uparrow,\ C_\downarrow)=(+1,\ 0)$.

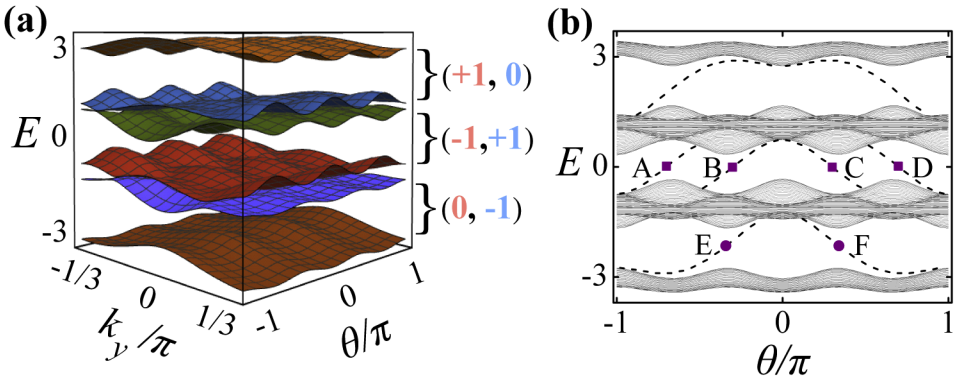

Fig. 2. Energy spectrum for $2\phi=0.6\pi$, $\Lambda=1.5$, $\beta=1/3$, $\Delta=1$, and $K=0.1$. The energy is set in units of J. (a) Energy spectrum $E=E(k_y,\theta)$ for the infinite BCL. The integers near the graph label the spin Chern numbers of different bandgaps. (b) Energy spectrum obtained from a finite ladder. As a function of θ, the spectrum is composed of the bulk bands (solid lines) and dispersion curves that traverse the gaps (dashed lines). ■ (•) is the markers for the states at the same Fermi energy.

The definite topological property in a finite system is the emergence of gapless edge states as the phase θ varies. In Fig. 2(b), illustrating the spectrum of a finite ladder, the dispersion curves of the additional states (dashed lines) are clearly superimposed on the bulk bandgaps. At a given Fermi level $E_{\text{Fermi}}=0$, gapless states, labeled as **A**, **B**, **C** and **D**, emerge in the middle bandgap. States **A** and **C** are localized near $n=L$, while **B** and **D** are localized near $n=0$ (Figs. 3(a)–3(d)). The slope of dispersion curves in Fig. 2(b) determines that the two states **A** and **C** are counterpropagating in the analogous 2D square lattice. Meanwhile, states **A** and **C** are almost fully spin-down and spin-up polarized, respectively (Figs. 3(a), 3(c)). Therefore, these two pair of mid-gap states form the helical edge states, indicating the QSHI phase of the middle gap. On the other hand, when the Fermi energy is adjusted inside the lowest gap, two propagating states traverse the bulk gap (**E** and **F** in Fig. 2(b)). **E** and **F** are characterized by

Optics EXPRESS

the single spin-component which are localized at the opposite edges (Fig. 3(e), 3(f)). In the analogous 2D system the excitations **E** and **F** constitute a pair of chiral edges states with single spin-component. This is associated with the spin-filtered QH phase [32,33]. We emphasize that the pseudospin components in our proposal are manifested as the leg degree of freedom. As a result, these edge states are localized at the extremities of the left- and right-legs, respectively. This will give convenience to the direct observations of the topological phases.

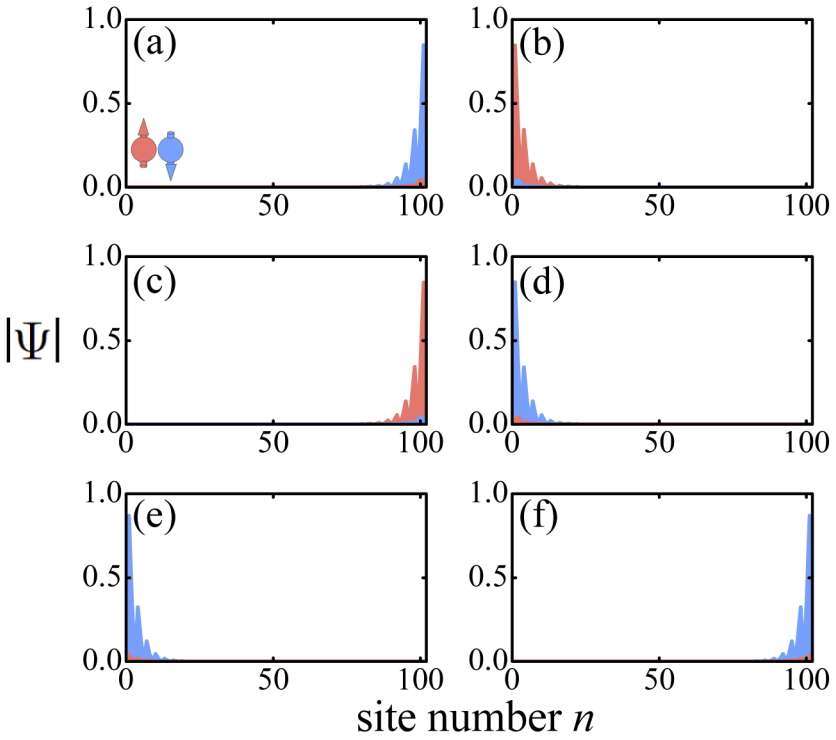

Fig. 3. Mode amplitudes of the gapless states in Fig. 2(b). (a-d) correspond to the states marked by ■, while (e,f) to the states •. The spin component $\Psi_{n\uparrow}$ (respectively, $\Psi_{n\downarrow}$) is represented in red (respectively, blue).

To further show the rich topological phases in the BCL, we explore the phase diagram through tuning the synthetic Hamiltonian. Since changing the energy offset between legs is readily accessible to the experiment, we compute the phase diagram as a function of the Δ. Figure 4 illustrates the diversity of the topological phases. The bulk is insulating in the white regions and classified into distinct phases: QH ($C_\uparrow = -1, C_\downarrow = -1$) or ($C_\uparrow = +1, C_\downarrow = +1$), QSH ($C_\uparrow = -1, C_\downarrow = +1$), spin-filtered QH ($C_\uparrow = \pm 1, C_\downarrow = 0$) or ($C_\uparrow = 0, C_\downarrow = \pm 1$), and ordinary insulator ($C_\uparrow = 0, C_\downarrow = 0$). Take $E_{\text{Fermi}} = 0$ and $E_{\text{Fermi}} = -1$ for example. With the increase of Δ the excitation of $E_{\text{Fermi}} = 0$ will undergo the regimes of metal, QSH insulator, and ordinary insulator successively. On the other hand, for the $E_{\text{Fermi}} = -1$ the energy offset can turn a QH phase into a metal, and then a spin-filtered QH phase. Therefore, by manipulating Δ and E_{Fermi} the BCL can host rich topological phases.

Optics EXPRESS

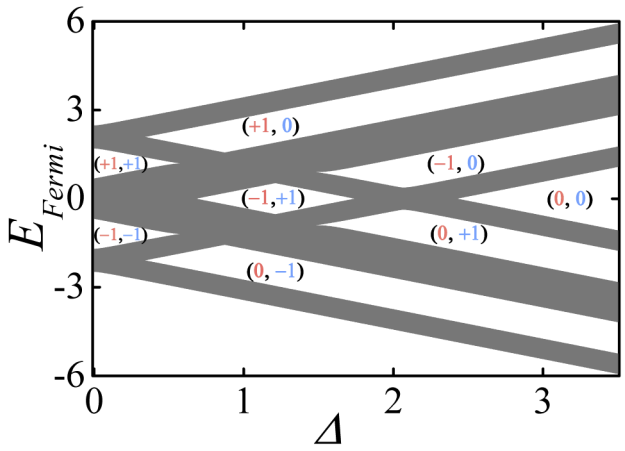

Fig. 4. E_{Fermi}-Δ phase diagram. Here, the bandgaps (bands) are designated by the white (shaded) regions, respectively. The pairs of integers indicate the Chern numbers of the bandgaps for spin up and down, distinguishing the topological regimes of the model.

4. Discussions and conclusions

One of the key features of our scheme is that the spinless ultracold atoms are utilized and the synthetic spin-orbit textures are built from the leg degree of freedom which is coupled to the Abelian gauge field. Neither internal states (e.g., hyperfine states) nor a non-Abelian gauge is used in our setting. Besides that, since the "spin" itself is synthesized in real space [11], our method allows for a real-space-resolved detection of the topological phases, instead of spin-resolved techniques. This character will facilitate greatly the direct observations of the spin-orbit coupled topological phases. On the other hand, due to the versatility of the optical ladders, we remark that our results are also applicable to the structures prepared in the artificial dimensions [12–20].

As an alternative to access the higher-dimensional Hamiltonians that host topological phases, the topological pumping in lower dimensional systems provides an additional avenue towards studying topological states of matter [24,34–38]. The pumping experiments of ultracold atoms have been demonstrated in optical superlattices [35,36]. Therefore, by adiabatically and periodically varying a set of BCLs' parameters, e.g., the relative phase of the bichromatic lattices, one can drive versatile quantized transports during each cycle, such as charge [34] and spin pumping [39]. The implementation of pumping in our BCL system will arouse the interest from the experimental side.

In conclusion, we have proposed a system of bichromatic chiral ladder for studying the topological bands for ultracold atoms, utilizing the concepts of synthetic spin-orbit coupling and Zeeman splitting. We have demonstrated that the quantum spin-Hall phase can emerge within this setup. In the meanwhile, the bichromatic chiral ladders can produce rich topological phases via tuning the system parameters. We conclude that the bichromatic chiral ladders hence constitute a surprisingly simple yet versatile scenario to explore synthetic topological quantum matter for the ultracold atoms. Our proposal to engineer topological quantum matter is of direct experimental relevance in ultracold atoms [11–13,19]. Taking this work as a basis, we believe that turning on the interactions will trigger the studies on the exotic topological many-body states in atomic chiral ladders [40–42].

Optics EXPRESS

Funding

National Natural Science Foundation of China (11574223, 11604231); Natural Science Foundation of Jiangsu Province (BK20150303, BK20160303); Natural Science Research of Jiangsu Higher Education Institutions of China (16KJB140012).

Disclosures

The authors declare no conflicts of interest.

References

1. N. R. Cooper, J. Dalibard, and I. B. Spielman, "Topological bands for ultracold atoms," Rev. Mod. Phys. **91**(1), 015005 (2019).
2. D. W. Zhang, Y. Q. Zhu, Y. X. Zhao, H. Yan, and S. L. Zhu, "Topological quantum matter with cold atoms," Adv. Phys. **67**(4), 253–402 (2018).
3. M. Atala, M. Aidelsburger, J. Barreiro, D. Abanin, T. Kitagawa, E. Demler, and I. Bloch, "Direct measurement of the Zak phase in topological Bloch bands," Nat. Phys. **9**(12), 795–800 (2013).
4. M. Aidelsburger, M. Lohse, C. Schweizer, M. Atala, J. T. Barreiro, S. Nascimbéne, N. R. Cooper, I. Bloch, and N. Goldman, "Measuring the Chern number of Hofstadter bands with ultracold bosonic atoms," Nat. Phys. **11**(2), 162–166 (2015).
5. M. Aidelsburger, M. Atala, M. Lohse, J. T. Barreiro, B. Paredes, and I. Bloch, "Realization of the Hofstadter Hamiltonian with Ultracold Atoms in Optical Lattices," Phys. Rev. Lett. **111**(18), 185301 (2013).
6. H. Miyake, G. Siviloglou, C. Kennedy, W. Burton, and W. Ketterle, "Realizing the Harper Hamiltonian with Laser-Assisted Tunneling in Optical Lattices," Phys. Rev. Lett. **111**(18), 185302 (2013).
7. G. Jotzu, M. Messer, R. Desbuquois, M. Lebrat, T. Uehlinger, D. Greif, and T. Esslinger, "Experimental realization of the topological Haldane model with ultracold fermions," Nature **515**(7526), 237–240 (2014).
8. S.-L. Zhu, H. Fu, C.-J. Wu, S.-C. Zhang, and L.-M. Duan, "Spin Hall Effects for Cold Atoms in a Light-Induced Gauge Potential," Phys. Rev. Lett. **97**(24), 240401 (2006).
9. N. Goldman, I. Satija, P. Nikolic, A. Bermudez, M. A. Martin-Delgado, M. Lewenstein, and I. B. Spielman, "Realistic Time-Reversal Invariant Topological Insulators with Neutral Atoms," Phys. Rev. Lett. **105**(25), 255302 (2010).
10. G. Velasco and B. Paredes, "Classification of topological ladder models," arXiv:1907.11460.
11. M. Atala, M. Aidelsburger, M. Lohse, J. T. Barreiro, B. Paredes, and I. Bloch, "Observation of chiral currents with ultracold atoms in bosonic ladders," Nat. Phys. **10**(8), 588–593 (2014).
12. M. Mancini, G. Pagano, G. Cappellini, L. Livi, M. Rider, J. Catani, C. Sias, P. Zoller, M. Inguscio, M. Dalmonte, and L. Fallani, "Observation of chiral edge states with neutral fermions in synthetic Hall ribbons," Science **349**(6255), 1510–1513 (2015).
13. B. Stuhl, H. I. Lu, L. Aycock, D. Genkina, and I. Spielman, "Visualizing edge states with an atomic Bose gas in the quantum Hall regime," Science **349**(6255), 1514–1518 (2015).
14. M. L. Wall, A. P. Koller, S. Li, X. Zhang, N. R. Cooper, J. Ye, and A. M. Rey, "Synthetic Spin Orbit Coupling in an Optical Lattice Clock," Phys. Rev. Lett. **116**(3), 035301 (2016).
15. L. Livi, G. Cappellini, M. Diem, L. Franchi, C. Clivati, M. Frittelli, F. Levi, D. Calonico, J. Catani, M. Inguscio, and L. Fallani, "Synthetic Dimensions and Spin-Orbit Coupling with an Optical Clock Transition," Phys. Rev. Lett. **117**(22), 220401 (2016).
16. S. Kolkowitz, S. L. Bromley, T. Bothwell, M. L. Wall, G. E. Marti, A. P. Koller, X. Zhang, A. M. Rey, and J. Ye, "Spin-orbit-coupled fermions in an optical lattice clock," Nature (London) **542**(7639), 66–70 (2017).
17. F. A. An, E. J. Meier, and B. Gadway, "Direct observation of chiral currents and magnetic reflection in atomic flux lattices," Sci. Adv. **3**(4), e1602685 (2017).
18. H. Cai, J. Liu, J. Wu, Y. He, S. Y. Zhu, J. X. Zhang, and D. W. Wang, "Experimental Observation of Momentum-Space Chiral Edge Currents in Room-Temperature Atoms," Phys. Rev. Lett. **122**(2), 023601 (2019).
19. J. H. Kang, J. H. Han, and Y. Shin, "Realization of a cross-linked chiral ladder with neutral fermions in an optical lattice by orbital-momentum coupling," Phys. Rev. Lett. **121**(15), 150403 (2018).
20. J. H. Han, J. H. Kang, and Y. Shin, "Band Gap Closing in a Synthetic Hall Tube of Neutral Fermions," Phys. Rev. Lett. **122**(6), 065303 (2019).
21. D. Hügel and B. Paredes, "Chiral ladders and the edges of quantum Hall insulators," Phys. Rev. A **89**(2), 023619 (2014).
22. G. Roati, C. D'Errico, L. Fallani, M. Fattori, C. Fort, M. Zaccanti, G. Modugno, M. Modugno, and M. Inguscio, "Anderson localization of a non-interacting Bose Einstein condensate," Nature **453**(7197), 895–898 (2008).
23. M. Modugo, "Exponential localization in one-dimensional quasi-periodic optical lattices," New J. Phys. **11**(3), 033023 (2009).
24. Y. E. Kraus, Y. Lahini, Z. Ringel, M. Verbin, and O. Zilberberg, "Topological States and Adiabatic Pumping in Quasicrystals," Phys. Rev. Lett. **109**(10), 106402 (2012).

Optics EXPRESS

25. L. J. Lang, X. Cai, and S. Chen, "Edge States and Topological Phases in One-Dimensional Optical Superlattices," Phys. Rev. Lett. **108**(22), 220401 (2012).
26. M. Verbin, O. Zilberberg, Y. E. Kraus, Y. Lahini, and Y. Silberberg, "Observation of Topological Phase Transitions in Photonic Quasicrystals," Phys. Rev. Lett. **110**(7), 076403 (2013).
27. Y. E. Kraus, Z. Ringel, and O. Zilberberg, "Four-Dimensional Quantum Hall Effect in a Two-Dimensional Quasicrystal," Phys. Rev. Lett. **111**(22), 226401 (2013).
28. Y. E. Kraus and O. Zilberberg, "Quasiperiodicity and topology transcend dimensions," Nat. Phys. **12**(7), 624–626 (2016).
29. P. G. Harper, "Single Band Motion of Conduction Electrons in a Uniform Magnetic Field," Proc. Phys. Soc., London, Sect. A **68**(10), 874–878 (1955).
30. D. Hofstadter, "Energy levels and wave functions of Bloch electrons in rational and irrational magnetic fields," Phys. Rev. B **14**(6), 2239–2249 (1976).
31. Y. Yang, Z. Xu, L. Sheng, B. Wang, D. Y. Xing, and D. N. Sheng, "Time-reversal-symmetry-broken quantum spin Hall effect," Phys. Rev. Lett. **107**(6), 066602 (2011).
32. N. Goldman, W. Beugeling, and C. Smith, "Topological phase transitions between chiral and helical spin with spin-orbit coupling and a magnetic field-tight binding," Europhys. Lett. **97**(2), 23003 (2012).
33. W. Beugeling, N. Goldman, and C. M. Smith, "Topological phases in a two-dimensional lattice: Magnetic field versus spin-orbit coupling," Phys. Rev. B **86**(7), 075118 (2012).
34. D. J. Thouless, "Quantization of particle transport," Phys. Rev. B **27**(10), 6083–6087 (1983).
35. M. Lohse, C. Schweizer, O. Zilberberg, M. Aidelsburger, and I. Bloch, "A Thouless Quantum Pump with Ultracold Bosonic Atoms in an Optical Superlattice," Nat. Phys. **12**(4), 350–354 (2016).
36. S. Nakajima, T. Tomita, S. Taie, T. Ichinose, H. Ozawa, L. Wang, M. Troyer, and Y. Takahashi, "Topological Thouless pumping of ultracold fermions," Nat. Phys. **12**(4), 296–300 (2016).
37. M. Lohse, C. Schweizer, H. M. Price, O. Zilberberg, and I. Bloch, "Exploring 4D quantum Hall physics with a 2D topological charge pump," Nature **553**(7686), 55–58 (2018).
38. O. Zilberberg, S. Huang, J. Guglielmon, M. Wang, K. P. Chen, Y. E. Kraus, and M. C. Rechtsman, "Photonic topological boundary pumping as a probe of 4D quantum Hall physics," Nature **553**(7686), 59–62 (2018).
39. L. Fu and C. Kane, "Time reversal polarization and a Z_2 adiabatic spin pump," Phys. Rev. B **74**(19), 195312 (2006).
40. S. Greschner, M. Piraud, F. Heidrich-Meisner, I. P. McCulloch, U. Schollwöck, and T. Vekua, "Spontaneous Increase of Magnetic Flux and Chiral-Current Reversal in Bosonic Ladders: Swimming against the Tide," Phys. Rev. Lett. **115**(19), 190402 (2015).
41. M. C. Strinati, E. Cornfeld, D. Rossini, S. Barbarino, M. Dalmonte, R. Fazio, E. Sela, and L. Mazza, "Laughlin-like States in Bosonic and Fermionic Atomic Synthetic Ladders," Phys. Rev. X **7**(2), 021033 (2017).
42. J. Jünemann, A. Piga, S. J. Ran, M. Lewenstein, M. Rizzi, and A. Bermudez, "Exploring Interacting Topological Insulators with Ultracold Atoms: The Synthetic Creutz-Hubbard Model," Phys. Rev. X **7**(3), 031057 (2017).